Biogeosciences

Open Access

EGU

Supplement of

Lateral carbon fluxes and CO$_2$ outgassing from a tropical peat-draining river

D. Müller et al.

Correspondence to: D. Müller (dmueller@iup.physik.uni-bremen.de)

1   Headspace method

For the determination of CO_2 in the water, a 600 ml flask was completely filled with water. A headspace of ambient air was introduced afterwards by pouring half the water out. The flask was then closed and the lid was connected to the CO_2 analyzer. The air was sampled from the headspace and pumped back into the water, forcing the air to bubble through the water, which accelerated the equilibration process. The principle is equivalent to that of headspace equilibration by shaking.

Water pCO_2 was calculated according to

$$pCO_2^{water,i} \approx pCO_2^{headspace,f} + \frac{V_h}{V_w}(pCO_2^{headspace,f} - pCO_2^{headspace,i})/(K_0RT),$$

where the indices i and f refer to initial and final pCO_2 (atm), V_h refers to the headspace volume and V_w refers to the water volume (in L). K_0 is the solubility of CO_2 in water calculated according to Weiss (1974), and converted to units of mol m^{-3} Pa^{-1}, R refers to the universal gas constant (8.314 J mol^{-1} K^{-1}) and T is the absolute temperature (in K). The initial pCO_2 was taken as the CO_2 measured in ambient air directly before the headspace equilibration measurement, the final pCO_2 was the equilibrium pCO_2 in the headspace. This formula is a good approximation in an acidic environment, because at a pH of 3.7-3.8, CO_2 accounts for >99% of DIC.

We are aware that the pH in the water may change when CO_2 is removed from the water, which is true for any method, where a discrete sample of water is brought to equilibrium with a headspace. However, in this environment, the acidity of the water is owed primarily to organic acids and not to carbonic acid, which is why we assume that the pH change during equilibration is negligible.

Figure S1: Sketch of the headspace equilibration technique used in this study.
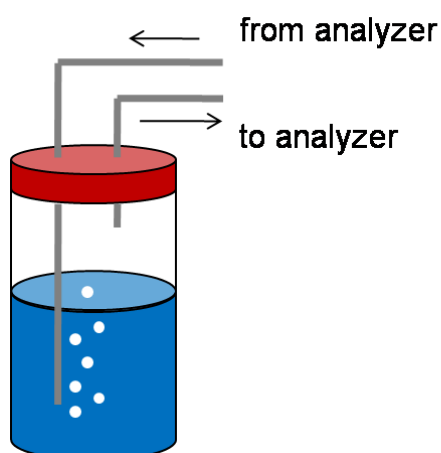
2   Scaling factor for Contros data

The Contros HydroC CO_2 Flow Through Sensor is only calibrated up to 1500 µatm CO_2. In lab experiments (December and March 2015, unpublished), we found that the instrument is nonlinear outside this range and underestimates CO_2 at high concentrations. Therefore, we conducted additional headspace measurements in the field using a 10 L container and a 200 ml headspace and measured the equilibrium pCO_2 with the Li-820. The correction described in (1) was not necessary, because the headspace volume to water volume ratio is very small. We found that on average, the pCO_2 was underestimated by 9 % (Figure S2). Therefore, we scaled the Contros data with a factor of 1.09. Note that this scaling factor is only appropriate for the concentrations measured in the field (ca. 7500-9000 µatm).

Figure S2: Figure displaying the Contros data scaled and unscaled, respectively, and the headspace measurements with the Li-820.
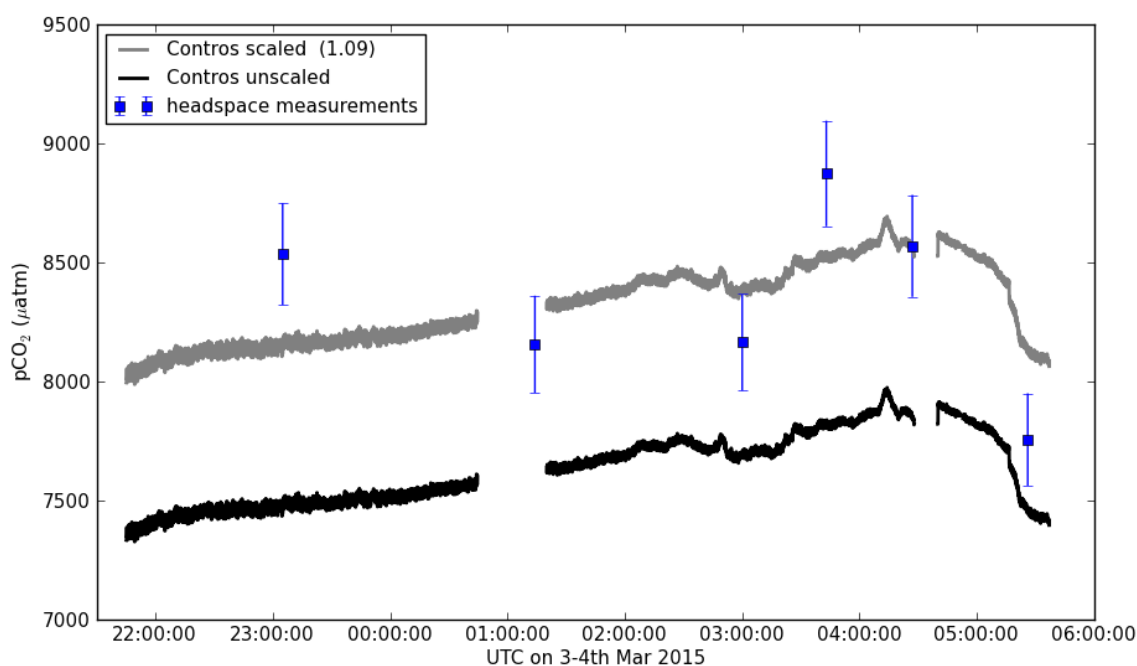
3 Gas exchange velocity calculations

Table S1. Calculation of the gas exchange velocity with seven equations from Raymond *et al.* (2012). The k_{600} values are in the unit cm/h. For the evaluation of the equations, we used V = 0.2 m/s, S = 0.00104, Q = 3.9 m³/s (4.4 m³/s) and D = 4 m.

Equation	Result (cm/h)
$k_{600} = ((VS)^{0.89} \cdot D^{0.54} \cdot 5037) \cdot 100/24$	23.5
$k_{600} = (5937 \cdot (1 - 2.54 \cdot Fr^2) \cdot (VS)^{0.89} \cdot D^{0.58}) \cdot 100/24$	29.2
$k_{600} = (1162 \cdot S^{0.77} \cdot V^{0.85}) \cdot 100/24$	6.2
$k_{600} = ((VS)^{0.76} \cdot 951.5) \cdot 100/24$	6.3
$k_{600} = (VS \cdot 2841 + 2.02) \cdot 100/24$	10.9
$k_{600} = (929 \cdot (VS)^{0.75} \cdot Q^{0.011}) \cdot 100/24$	6.8
$k_{600} = (4725 \cdot (VS)^{0.86} \cdot Q^{-0.14} \cdot D^{0.66}) \cdot 100/24$	27.7 (27.3)

4   Carbon yield calculations and uncertainties

Table S2: Calculations of TOC yield, CO_2 yield and % CO_2 of combined TOC+CO_2 yield. Q refers to discharge, C_{TOC} to the TOC concentration, A to the catchment area, F_g to the flux in gC m^{-2} d^{-1}.

Parameter	Formula	Units	Result
TOC yield	$TOCyield = Q \cdot C_{TOC}/A$	gC/m2catchment area/yr	
CO_2 yield	$CO_2yield = F_g \cdot 0.89\% \cdot A/A \cdot 365$	gC/m2 catchment area/yr	
	$CO_2yield = F_g \cdot 0.89\% \cdot A/A \cdot 365$		
% CO_2 outgassing of combined yield	$\%CO_2yield = CO_2yield/ (CO_2yield + TOCyield)$	%	

Table S3: Summary of the treatment of uncertainties when calculating the TOC and CO_2 yield.

Parameter	Variable	Uncertainty estimate
TOC yield	Q	We used three ET estimates from the literature (see text) and calculated three Q estimates from it. For our calculations, we used the average. The uncertainty is taken as the largest deviation of a single Q value from this average.
	C_{TOC}	We used the standard deviations of the 2014 and 2015 medians as uncertainty.
	A	The HydroSHEDS have a spatial resolution of 30 sec, therefore, we used ~1 km as spatial uncertainty and 1 km² as uncertainty of the catchment area.
CO_2 yield	F_g	For the flux, the uncertainty was calculated from the propagation of the uncertainties associated with the gas exchange velocity (as represented by the standard deviation) and the pCO$_2$ (which was assumed to be 2.5% according to the headspace method).
	0.89%	The stream coverage for Indonesia is, according to Raymond et al. (2013), 0.73%. The deviation of these two values (0.16%) was taken as uncertainty.

5   Radiocarbon age determination

Figure S3: Calendar age calibration curve (green) and probability distribution for the calendar age of sample SGM02 (106.59 ± 0.32 pMC). Light blue are one sigma intervals, dark blue are two sigma intervals. The figure was generated using the post-bomb calibration program CALIBomb (Reimer *et al.*, 2004) (available at http://calib.qub.ac.uk/CALIBomb/) with the atmospheric radiocarbon timeseries from Reimer *et al.* (2013) and the bomb curve extension NHZ3 (Hua *et al.,* 2013). It can be seen that two solutions are possible: One before the main bomb peak and one after. We consider the more recent sample age more likely, because the peat in our study area is intact.
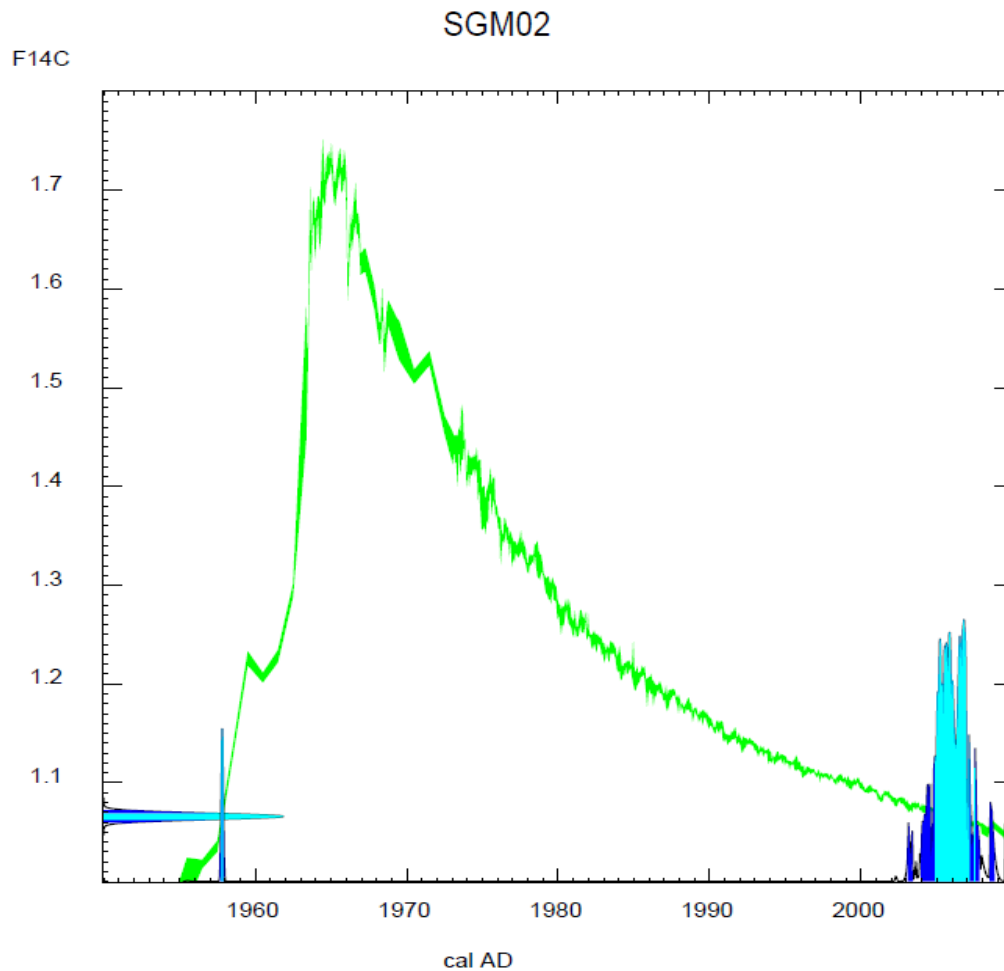
6   References

Hua, Q., Barbetti, M. and Rakowski, A. Z.: Atmospheric Radiocarbon for the Period 1950-2010. Radiocarbon 55 (4): 2059-2072, 2013.

Raymond, P. A.; Zappa, C. J.; Butman, D.; Bott, T. L.; Potter, J. D.; Mulholland, P.; Laursen, A. E.; McDowell, W. H. and Newbold, D.: Scaling the gas transfer velocity and hydraulic geometry in streams and small rivers. Limnology and Oceanography: Fluids and Environments 2: 41-53, 2012.

Reimer P. J., Bard E., Bayliss A., Beck J.W., Blackwell P. G., Bronk Ramsey C., Buck C. E., Cheng H., Edwards R. L., Friedrich M., Grootes P. M., Guilderson T. P., Haflidason H., Hajdas I., Hatté C., Heaton T. J., Hogg A. G., Hughen K. A., Kaiser K. F., Kromer B., Manning S. W., Niu M., Reimer R. W., Richards D. A., Scott E. M., Southon J. R., Turney C. S. M., van der Plicht J.: IntCal13 and MARINE13 radiocarbon age calibration curves 0-50000 years calBP. Radiocarbon 55(4), 2013.

Reimer, P. J., Brown, T. A., and Reimer, R. W. Discussion: Reporting and Calibration of Post-Bomb ^{14}C Data. Radiocarbon 46 (3): 1299-1304, 2004.